Global Climate Projections, Sea Level Rise, and Extreme Precipitation: Final report to the Port Gamble S'Klallam Tribe

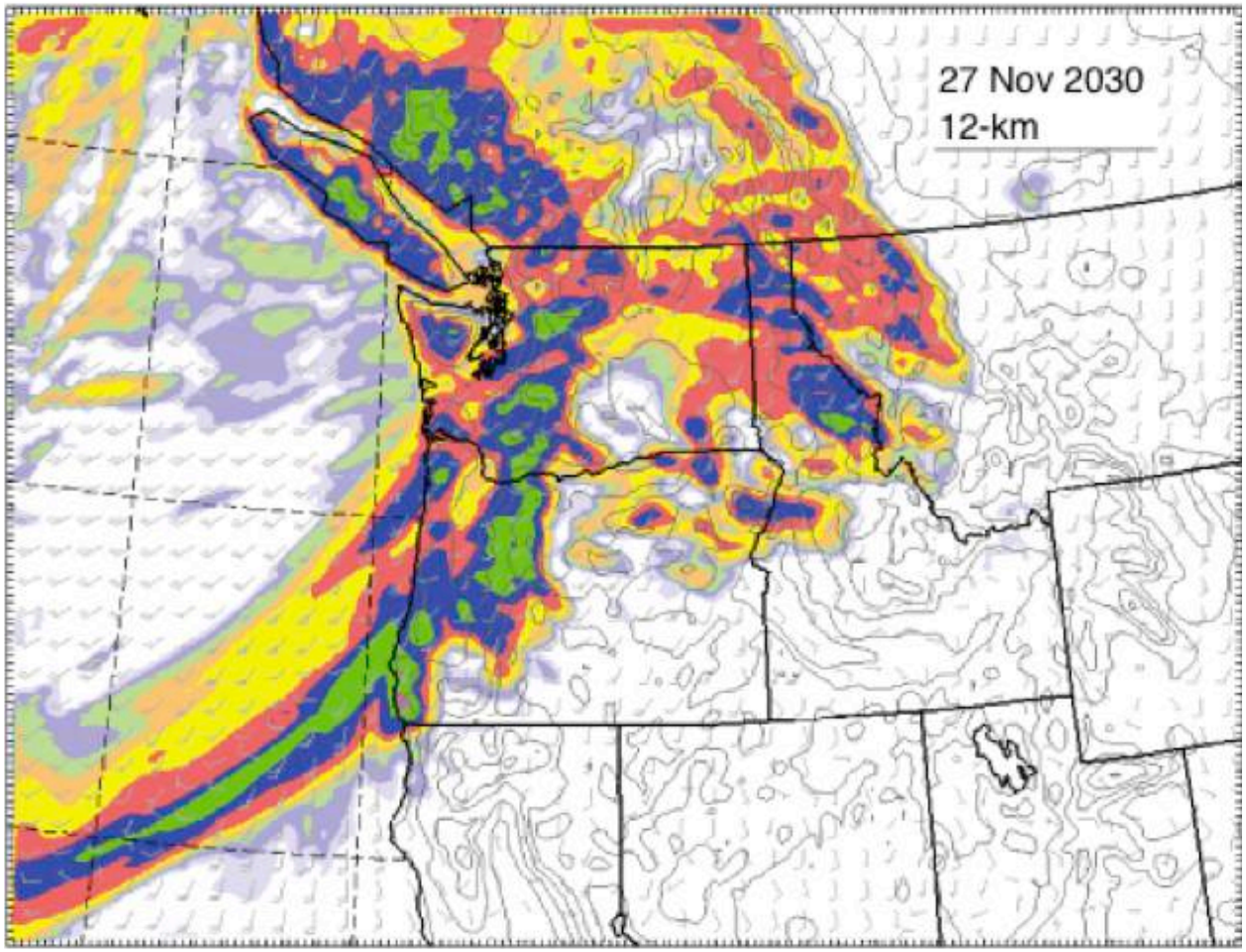

Prepared by the

Climate Impacts Group | University of Washington

April 2018

Guillaume Mauger, University of Washington, Climate Impacts Group
Katherine Hegewisch, Univerisity of Idaho, Department of Geography
Ian Miller, Washington Sea Grant
Jason Won, University of Washington, Climate Impacts Group
Cary Lynch, Joint Global Change Research Institute

Cover image: Future storm projected by the regional climate model used in this study (Source: Eric Salathé, University of Washington)

Acknowledgements

The authors would like to thank Rick Steed for his help in producing the GFDL WRF simulation used in this report, as well as Cliff Mass for his generous donation of computing resources. Robert Norheim produced the interactive online visualizations using Tableau. This project was funded by the Port Gamble S'Klallam Tribe via a contract with Cascadia Consulting.

Recommended Citation

Mauger, G.S., K. Hegewisch, I.M. Miller, J.S. Won, C. Lynch, 2018. Global Climate Projections, Sea Level Rise, and Extreme Precipitation: Final report to the Port Gamble S'Klallam Tribe. Climate Impacts Group, University of Washington, Seattle.

Errata

The following errors have been identified and corrected since the initial publication of this report:

October 30th, 2018

Correction to text on page 19. Previous text made incorrect references to tables and results.

New text: *"As Table 5 suggests, the models do not correspond to the extremes among all GCMs and scenarios for all metrics and all times. In fact, the models do not generally correspond to their 'Low' and 'High' designations, which were based on an analysis of the regional drivers of precipitation. This is likely due to the distinct micro-climate of the northeast Olympic peninsula."*

Previous text: *"As Table 3 suggests, the models do tend to correspond to their 'Low' and 'High' titles for the winter and water year statistics. Since the largest atmospheric rivers tend to occur in winter, this is appropriate. In other seasons, the GFDL projection tends to be higher, but the results are more mixed. As Figures 3 and 4 suggest, the two bracketing models will not correspond to the extremes among all GCMs and scenarios for all metrics and all times."*

Table of Contents

About this Report

This report describes the results of Tasks B-D in the attached scope of work (Appendix A). Other tasks (Tasks A, E, and F) are covered in separate reports (Port Gamble S'Klallam Tribe, 2017; Ramirez and Simenstad, 2018). The specific objectives tasks B-D were:

Task B. Synthesize and statistically downscale global climate model projections.

This task had two parts:

1. Synthesize global model projections. Specifically, the Tribe was interested in evaluating climate projections through the year 2160 (which spans seven generations).
2. Statistically downscale global climate model projections. The purpose of this task is to produce downscaled climate change projections for areas of interest to the Tribe. This task leveraged recent work to apply a correction to existing statistically downscaled projections.

Task C. Produce local relative sea level rise projections.

As in Task B.1, the purpose of this task was to produce updated sea level rise projections through the year 2160. This work leverages the ongoing Washington Coastal Resilience Project (WCRP), funded by the NOAA Office of Coastal Resilience.

Task D. New projections of changing heavy precipitation.

The goal of this task was to produce new physically-based estimates of changing heavy precipitation. This task leveraged existing funding from King County to produce two new regional climate model simulations for the region.

This report describes the methods and products developed for each of these tasks, referencing other reports when results are leveraged from a larger parallel effort.

Task B.1: Synthesize Global Climate Model Projections

Background

Climate projections for Pacific Northwest temperature and precipitation are currently available in the existing literature (e.g., Mauger et al., 2015). However, few existing studies look beyond the year 2100. The purpose of this task is to synthesize existing global climate model projections through the year 2160 (approximately seven generations from present day).

Data & Methods

GCM projections were obtained from the Climate Model Inter-comparison Project, phase 5 (CMIP5; Taylor et al., 2012). As part of the CMIP5 project, international modeling groups coordinate to create a set of consistent future simulations, driven by predetermined greenhouse gas scenarios ("Representative Concentration Pathways", or RCPs, van Vuuren et al., 2011; for more on climate scenarios, see Section 1 of Mauger et al., 2015).

Although the primary focus of the CMIP5 project is to develop a consistent set of projections through the year 2100, van Vuuren et al. (2011) also developed a set of Extended Concentration Pathways (ECPs), based on the original four, that continue through 2300. Fewer GCMs include projections through this time frame, but there are nonetheless enough to develop robust estimates of future conditions past 2100.

Each GCM is often run multiple times for each greenhouse gas scenario, each time with slightly different initial conditions. Since the climate system is chaotic, the small changes in initial conditions result in a different sequence of weather and climate variability in each simulation. These are referred to as "realizations", since each of these simulations represents one possible sequence of events for the same boundary conditions – in the same way that a lab experiment might be repeated to determine if the results can be replicated.

Although many of the CMIP5 GCMs have multiple realizations, in this study we only used one realization for each model. We did this for two reasons: (1) especially over long time frames, differences between GCMs are more important than differences among separate realizations for a single GCM and (2) due to the limited scope of this study it was not feasible to include the additional data management and processing that would be needed to evaluate more than one realization for each GCM. For simplicity, we used the first realization of each model (labeled "r1" in the CMIP5 archive).

Models were chosen based on availability of monthly data. Table 1 includes a full list of the GCMs that were included in our analysis, and Table 2 lists the extended projections that were obtained for each greenhouse gas scenario. The number and selection of models differed for each greenhouse gas scenario. In particular, the CMIP5 project

prioritized the RCP 4.5 and 8.5 scenarios, since these are deemed representative of the low- and high-end of the plausible range in future greenhouse gas emissions. Only two models included projections beyond 2100 for the RCP 6.0 scenario; too small of a number to develop robust change estimates. On the low end, recent research suggests that the RCP 2.6 is not likely to be achievable, given current fossil fuel infrastructure and its expected lifetime. Although recent emissions have been closer to the RCP 8.5 scenario, this represents only the first ~10 years of a century-long scenario. Current research does not suggest that either the RCP 4.5 or RCP 8.5 scenario is more likely than the other.

Model	***Source***	***Resolution*** *(°lat x °lon)*	***Vertical Levels***
ACCESS1-0	Commonwealth Scientific and Industrial Research Organization, Australia/ Bureau of Meteorology, Australia	1.25 x 1.88	38
ACCESS1-3	Commonwealth Scientific and Industrial Research Organization, Australia/ Bureau of Meteorology, Australia	1.25 x 1.88	38
bcc-csm1-1	Beijing Climate Center, China Meteorological Administration	2.8 × 2.8	26
bcc-csm1-1-m	Beijing Climate Center, China Meteorological Administration	1.12 × 1.12	26
BNU-ESM	College of Global Change and Earth System Science, Beijing Normal University, China	2.8 × 2.8	26
CanESM2	Canadian Centre for Climate Modeling and Analysis	2.8 × 2.8	35
CCSM4	National Center of Atmospheric Research, USA	0.94 × 1.25	26
CESM1-BGC	Community Earth System Model Contributors	0.94 × 1.25	26
CESM1-CAM5	Community Earth System Model Contributors	0.94 × 1.25	26
CNRM-CM5	National Centre of Meteorological Research, France	1.4 × 1.4	31
CSIRO-Mk3-6-0	Commonwealth Scientific and Industrial Research Organization/ Queensland Climate Change Centre of Excellence, Australia	1.8 × 1.8	18
FGOALS-g2	LASG, Institute of Atmospheric Physics, Chinese Academy of Sciences	2.8 × 2.8	26
FIO-ESM	First Institution of Oceanography, State Oceanographic Administration (SAO), Qingdao, China	2.8 x 2.8	26
GFDL-CM3	NOAA Geophysical Fluid Dynamics Laboratory, USA	2.0 × 2.5	48
GFDL-ESM2G	NOAA Geophysical Fluid Dynamics Laboratory, USA	2.0 × 2.5	24
GFDL-ESM2M	NOAA Geophysical Fluid Dynamics Laboratory, USA	2.0 × 2.5	24

GISS-E2-H	NASA Goddard Institute for Space Studies, USA	2.0 × 2.5	40
GISS-E2-R	NASA Goddard Institute for Space Studies, USA	2.0 × 2.5	40
HadGEM2-AO	Met Office Hadley Center, UK	1.25 × 1.88	38
HadGEM2-CC	Met Office Hadley Center, UK	1.25 × 1.88	60
HadGEM2-ES	Met Office Hadley Center, UK	1.25 × 1.88	38
inmcm4	Institute for Numerical Mathematics, Russia	1.5 × 2.0	21
IPSL-CM5A-MR	Institut Pierre Simon Laplace, France	1.25 × 2.5	39
MIROC5	Atmosphere and Ocean Research Institute (The University of Tokyo), National Institute for Environmental Studies, and Japan Agency for Marine-Earth Science and Technology	1.4 × 1.4	40
MIROC-ESM	Japan Agency for Marine-Earth Science and Technology, Atmosphere and Ocean Research Institute (The University of Tokyo), and National Institute for Environmental Studies.	2.8 × 2.8	80
MIROC-ESM-CHEM	Japan Agency for Marine-Earth Science and Technology, Atmosphere and Ocean Research Institute (The University of Tokyo), and National Institute for Environmental Studies.	2.8 × 2.8	80
MPI-ESM-LR	Max Planck Institute for Meteorology, Germany	1.87 × 1.88	47
MPI-ESM-MR	Max Planck Institute for Meteorology, Germany	1.87 × 1.88	95
MRI-CGCM3	Meteorological Research Institute, Japan	1.1 × 1.1	48
MRI-ESM1	Meteorological Research Institute, Japan	1.1 × 1.1	50
NorESM1-M	Norwegian Climate Center, Norway	1.9 × 2.5	26
NorESM1-ME	Norwegian Climate Center, Norway	1.9 × 2.5	26

Table 1. Global Climate Models that were evaluated for this study. Note that many institutions include several versions of their model in the Coupled Model Intercomparison Project (CMIP) archive. All models are relatively coarse in spatial resolution, but the spacing varies substantially among models. For more on climate scenarios, see Section 1 of Mauger et al. (2015).

CMIP5 historical simulations are used to calculate the change relative to a historical baseline. Since each model may simulate the climate differently, it is important to evaluate a model's future climate relative to the same model's historical simulation. Since start dates vary by model and our emphasis is on future conditions relative to the

GCM	*Very Low (RCP 2.6)*	*Low (RCP 4.5)*	*Moderate (RCP 6.0)*	*High (RCP 8.5)*
bcc-csm1-1	X	X		X
CanESM2	X	X		
CCSM4	X	X	X	X
CESM1-CAM5	X	X	X	
CNRM-CM5		X		X
CSIRO-Mk3-6-0		X		X
FGOALS-g2		X		
GFDL-ESM2G		X		X
GISS-E2-H	X	X		X
GISS-E2-R	X	X		X
HadGEM2-ES	X	X		X
IPSL-CM5A-MR		X		
MIROC-ESM		X		
MPI-ESM-LR	X	X		X
NorESM1-M		X		

Table 2. Global climate model projections that were obtained for each greenhouse gas scenario. The table includes the subset of CMIP5 models for which extended projections are available, noting which projections were obtained for each of the four greenhouse gas scenarios. The greatest number of projections were available for the low-end RCP 4.5 scenario.

recent past, we evaluated simulations from the last half of the 20th century (1950-1999) only.

The future CMIP5 simulations begin in 2006, the start year for the greenhouse gas scenarios. Most extended simulations continue through 2300, though some end as early as 2200. For all extended scenarios, we obtained data through 2160 (Table 2). For those models that did not include an extended scenario, we included the projections through 2100.

Projections were synthesized into annual (Jan-Dec) or seasonal averages (Dec-Feb, Mar-May, Jun-Aug, Sep-Nov). Since models differ substantially in terms of their absolute temperature and precipitation estimates, for this work we focused on the change relative to the average for 1950-1999. Specifically, for each year in every historical and future simulation, the seasonal and annual average temperature difference (in °C) is calculated relative to the average for 1950-1999. The same is done for precipitation, except that the percent change is calculated.

The ensemble average across all models is calculated from all available data for a particular scenario and year. If less than five models are available for a particular scenario and year, an average is not computed.

Results

The results of the climate change projections are made available via an interactive online tool (Figure 1). The tool can be accessed at the following URL:

https://doi.org/10.5072/FK2PC32811

The interactive viewer allows users to select the future time frame (or the number of generations), season, and greenhouse gas scenario for the future projections. Models can be viewed one at a time, all at once, or only those models for which extended projections are available (Table 2). All of the projections that are included in the tool are also available in a spreadsheet, which can be obtained by clicking the “download” button on the bottom right of the screen.

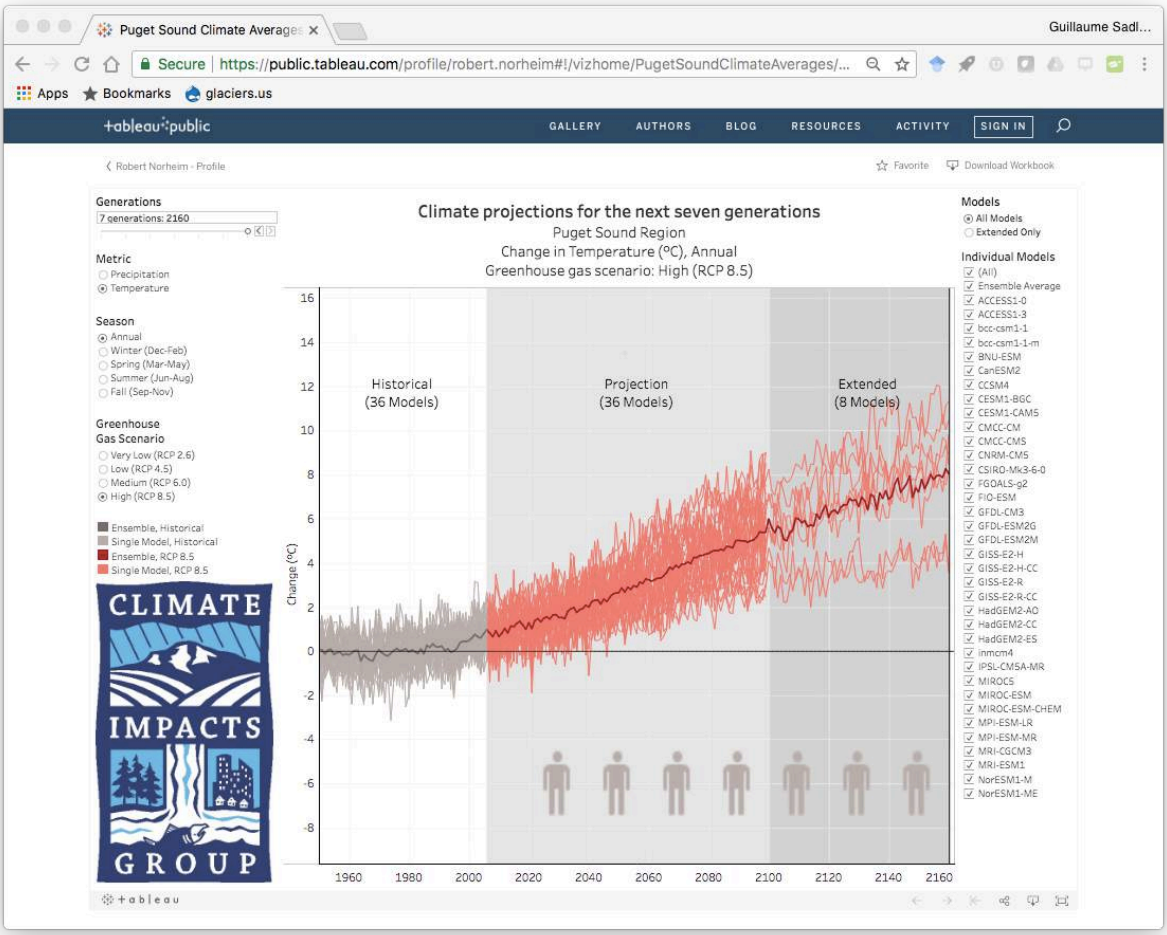

Figure 1. Screenshot of the interactive tool. Available online at: https://doi.org/10.5072/FK2PC32811

Task B.2: Statistically Downscaled Projections

Background

Global climate models are coarse in spatial resolution: they do not resolve local-scale variations in topography, land cover, or the associated implications for local weather and climate. "Downscaling" is the term used for approaches that relate large-scale conditions from global climate models to local-scale variations in climate (for more on downscaling, see Section 1 of Mauger et al., 2015). Statistical downscaling is an empirical approach, based on statistical relationships between surface weather observations and coarse-scale GCM weather patterns.

Surface weather observations – in particular long-term high-quality records – are typically sparse in spatial coverage, and tend to be biased towards low elevation areas near population centers. As a result, numerous approaches have been developed to produce spatially distributed and temporally complete estimates of daily temperature, precipitation, and winds for use in driving hydrologic model simulations (e.g., Maurer et al., 2002, Daly et al., 2002, Di Luzio et al., 2008, Hamlet and Lettenmaier 2005, Hamlet et al., 2013, Livneh et al., 2013, 2015). Although the methods vary, the general approach is to interpolate weather observations onto a grid and then apply corrections based on proximity and topographic similarity.

Recent evaluations of the Livneh et al. (2013) dataset have shown that the fixed lapse rate assumption (used for estimating temperature change with elevation) can result in substantial biases, since most observations are at low elevation and the atmosphere can deviate significantly from this rate of temperature change with altitude. In particular, temperatures at elevation can exhibit a substantial cold bias in the winter months. Temperature biases are largest in the mountains, where the fixed lapse rate assumption is particularly ill-suited (for more on these biases, see Mauger et al., 2016).

Since gridded meteorological datasets such as Livneh et al. (2013) are the basis for statistically downscaled projections, these biases can translate into errors in the estimated impacts of climate change. This is particularly true for hydrologic model simulations, since many elements of the water balance – snow accumulation and melt, evaporation, transpiration – depend non-linearly on temperature. The purpose of this task is to apply a correction to the Livneh dataset and an associated statistically downscaled set of projections, in order to provide improved estimates of future conditions in areas of interest to the PGSK Tribe. This effort leverages and builds on a previous effort described by Mauger et al. (2016).

Data & Methods

Gridded Historical and Future Climate Data

Gridded historical meteorological data were obtained from the 1/16-degree Livneh v1.1 dataset (version 15Oct2014, Livneh et al., 2015, http://www.colorado.edu/lab/livneh/data). The dataset includes daily estimates of minimum and maximum temperature, precipitation, and wind speed from Jan 1, 1950 to Dec 31, 2013.

The statistically downscaled projections were obtained from the MACAv2-LIVNEH dataset (Multivariate Adaptive Constructed Analogues, Hegewisch and Abatzoglou 2016, Abatzoglou and Brown 2012). As with all statistical downscaling approaches, MACA was applied by using an observationally-based dataset to develop empirical relationships between coarse-scale global model projections and local-scale weather and climate variations. In this case the dataset used was Livneh v1.0 (on the US side) and Livneh v1.1 on the Canadian side (Livneh et al., 2013). MACA was applied at the daily time step, and used a multivariate constructed analogues approach, meaning that a historical library of observations was used to relate similar meteorological states in both the GCM and the observations.

Projections are based on 10 global models from the CMIP5 (Coupled Model Intercomparison Project Phase 5, Taylor et al., 2012) experiment. The 10 GCMs were selected from the larger set of CMIP5 simulations based on their ability to accurately represent the climate of the Pacific Northwest (Rupp et al., 2013). The MACA downscaling was applied to the historical simulations (1950-2005) and two future projections (2006-2099) for each GCM (i.e., two time series per GCM). The two projections were taken from the low (RCP 4.5) and high (RCP 8.5) greenhouse gas scenarios (Van Vuuren et al., 2011). Although some of the GCMs evaluated in Task B.1 extend through 2160, it was beyond the scope of this study to extend the statistically downscaled projections beyond 2099.

Statistical Downscaling

We applied a correction to the gridded Livneh meteorological v1.0/v1.1 dataset using monthly data from the Parameter Regression on Independent Slopes Model (PRISM AN81M monthly, Daly et al., 2008). Since the Livneh dataset extends into Canada, a PRISM climatology developed for British Columbia (PCIC, 2014) was applied to the Canadian portion of the domain. To do this, the monthly U.S. PRISM data was aggregated from its 1/24-degree native resolution to the 1/16-degree Livneh grid. Similarly, the PRISM climatology from PCIC was aggregated from 1/120-degree to 1/16-degree resolution. Whereas the climatology was used in the Canadian portion of the domain, the PRISM monthly time series from Jan 1950 – Dec 2013 was used for the U.S. portion of the domain. Using the reference PRISM datasets, a simple bias adjustment was performed by adjusting the daily Livneh temperatures with the

difference between the monthly Livneh dataset and the interpolated monthly PRISM temperature variables. For precipitation, a ratio was used in lieu of a difference. The final result was that the Livneh dataset has the same monthly climatology as the PRISM dataset.

One additional correction was applied due to a complication in the method that arose for precipitation: when the monthly total in the Livneh dataset was zero but non-zero in the PRISM dataset, the consequence was an infinite ratio (divide by zero) for scaling the Livneh dataset. To avoid this, the daily precipitation data was simply scaled uniformly to match the PRISM monthly value instead of using a ratio. The resulting bias corrected training dataset ("bcLivneh") covers an area between 41 – 53 N and 125 to 108W for Jan 1, 1950 to Dec 31, 2013.

For consistency with the corrected Livneh et al. (2013) dataset, the MACA projections were also bias-adjusted so that the historical average for each month in the MACA data matched the same quantity in the PRISM data. Corrections to the MACA dataset were computed by applying the difference between the average monthly values for temperature from the Livneh NAmerExt dataset (1950-2013, equivalent to using PRISM) and the Livneh v1.0/v1.1 combination dataset (1950-2011). For precipitation, the ratio was used instead of the difference. These monthly corrections were applied to all daily values in each month of the MACAv2-LIVNEH dataset to correct both the historical and future values in the MACA projections.

Since hydrologic changes such as streamflow, snowpack, and evapotranspiration are often the primary impacts of interest, we ran the new meteorological datasets through an uncalibrated version of the Variable Infiltration Capacity (VIC) macroscale hydrologic model (Liang et al., 1994, Liang et al., 1996, Gao et al., 2010). We used VIC model version 4.1.2g, with the same soil, vegetation, and elevation parameter files as Hamlet et al. (2013).

Results

Although the focus of this work is the areas of interest to the PGSK Tribe, we developed the dataset for the entire Pacific Northwest domain, as this is the standard approach and it required minimal additional effort. The data are currently available for download online:

bcLivneh: http://cses.washington.edu/rocinante/Livneh/bcLivneh_WWA_2013

bcMACA: http://cses.washington.edu/rocinante/MACA/bc/

Results are stored both as individual files for each grid cell and zipped files containing results for the entire domain. The directory structure is illustrated in Figure 2. Meteorological data is contained in the "forcings" directory and associated zipped file, while the hydrologic model results are in the "fluxes" directory.

It is worth noting that for most watersheds in western Washington, the model is uncalibrated. Although more reliable estimates could be obtained by calibrating the model, these data are nonetheless provided as a first estimate of hydrologic variations in the region. We recommend using the current results to estimate the percent changes in hydrologic variables, relative to some historical baseline, as opposed to absolute estimates of basin hydrology.

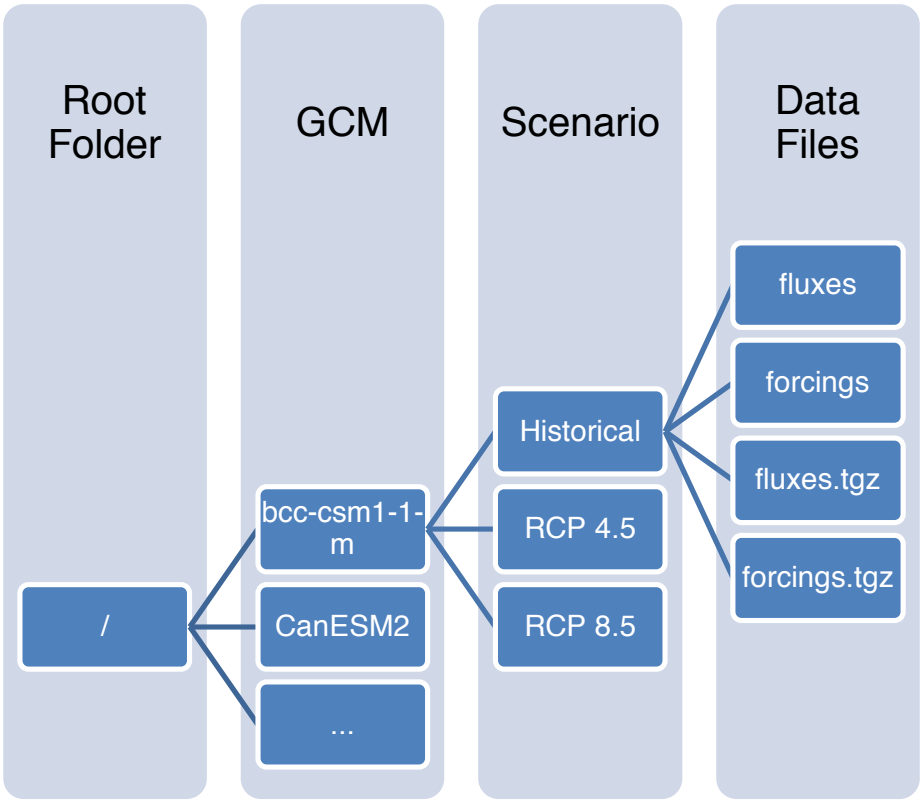

Figure 2. Data structure for the statistically downscaled bcMACA. The bcLivneh structure simply follows the "Data Files" column, since there are no GCMs and no scenarios.

Task C: Produce Local Relative Sea Level Rise Projections

Background

Observations show that sea level in the Pacific Northwest has risen by about 8 inches since 1900, and projections that several additional feet of sea level rise are possible by the end of the 21st century (e.g., see Section 4 in Mauger et al., 2015). However, existing sea level rise projections for the region have not been updated in light of new science, do not provide sub-regional specificity in impacts, and have not been effectively synthesized for use by managers.

This task leverages two recent efforts aimed at producing new community-scale projections of relative sea level rise for Washington State, funded by NOAA's Regional Coastal Resilience Grants Program and EPA's National Estuarine Program (via the Puget Sound Partnership). We refer to the combination of these sea level rise efforts as the Washington Coastal Resilience Project (WCRP). This section briefly describes the relative sea level rise projections that have been produced. Further information can be found in a forthcoming report describing the science and providing guidance on how to use the projections (e.g., Miller et al., 2018).

Data & Methods

In this work we differentiate between "absolute" sea level rise – which measures the change in sea surface height relative to a fixed reference frame (e.g., the center of the earth) – and "relative" sea level rise – which measures changes in the height of the surface relative to vertical motion of the land. In the tectonically-active Pacific Northwest, land movement can have a measurable effect on observed and projected relative sea level.

For WCRP we assessed absolute sea level and vertical land movement separately, and then combined them together to create relative sea level projections. Absolute sea level rise projections were developed following the methods described in Kopp et al. (2014). In this approach, the uncertainties in each component of sea level rise are combined to produce a set of probabilistic future projections for each greenhouse gas scenario. Since probabilities cannot be assigned to greenhouse gas scenarios (see Section 1 of Mauger et al., 2015), separate probabilistic projections are produced for each scenario.

The only deviation from the Kopp approach was in the estimated effect of Glacial Isostatic Adjustment (GIA, the response of the Earth's crust to the retreat of ice sheets from the last ice age) on absolute sea level rise. Since Kopp combined vertical land motion due to GIA with its effect on absolute sea level rise, we incorporated estimates of the absolute component only, obtained from NRC (2012). Additional information on GIA can be found in Miller et al. (2018).

For vertical land motion (VLM), we produced a new high-resolution dataset based on a combination of vertical rate estimates from multiple sources. Specifically, we combined vertical rate estimates obtained from continuous Global Positioning System (GPS) monitoring sites, benchmark leveling stations, tide gauges, and the results of a "locking model" representing crustal deformation due to the subducting Cascadia fault. These four datasets were combined into a single best estimate, plus uncertainty, in vertical land motion for each point on a 10 km grid covering all of western Washington State. The result is a probabilistic estimate of VLM for each point on Washington's coastline, which can then be easily integrated with the absolute sea level rise projections described above. Further details on the VLM estimates can be found in Appendix C of Miller et al. (2018).

Relative sea level rise projections are obtained by resampling from the probability distribution in absolute sea level rise projections, again in a monte carlo approach. For each iteration, estimates of absolute sea level rise and vertical land motion are randomly selected from each probability distribution, and combined. This process is repeated thousands of times, producing a probability distribution for relative sea level rise. The monte carlo approach is applied separately to each future decade and each greenhouse gas scenario.

Results

Year	Greenhouse Gas Scenario	Central Estimate (50%)	Likely Range (17-83%)	Higher magnitude, but lower likelihood possibilities		
				10% probability	1% probability	0.1% probability
2050	**RCP 4.5 (Low)**	0.7	0.4 – 1.0	1.1	1.5	2.0
	RCP 8.5 (High)	0.8	0.5 – 1.1	1.2	1.6	2.2
2100	**RCP 4.5 (Low)**	1.8	1.0 – 2.6	2.9	4.4	7.7
	RCP 8.5 (High)	2.2	1.4 – 3.1	3.4	5.1	8.6
2150	**RCP 4.5 (Low)**	2.8	1.5 – 4.3	4.9	8.9	16.6
	RCP 8.5 (High)	3.8	2.4 – 5.4	6.1	10.3	18.8

Table 3. Summary of relative sea level projections, in feet, relative to contemporary sea level for the the grid cell closest to the Port Gamble S'Klallam reservation (47.9N, 122.6W). Results are shown for both a low and a high greenhouse gas scenario (RCPs 4.5 and 8.5, respectively), and for three different time periods (2050, 2100, and 2150) across a range of probabilities. Projections for each year are actually based on a 19-year average of the projections, centered on each year. The text descriptors associated with probabilities are adapted from descriptors utilized by the Intergovernmental Panel on Climate Change.[1]

[1] See https://www.ipcc.ch/pdf/supporting-material/uncertainty-guidance-note.pdf

Relative sea level rise projections for the point closest to the PGSK Tribal Center are shown in Table 3. These were obtained by extracting specific percentiles from the probability distributions of relative sea level rise described in the previous section. Additional projections, for all of Washington State, will be provided in forthcoming reports, guidance, and data products developed as part of the Washington Coastal Resilience Project.

Task D: New Projections of Changing Heavy Precipitation

Background

Changes in the intensity, duration, and frequency of precipitation may negatively affect stormwater facilities, exacerbate landslide and urban flood risk, and lead to other public safety and water quality concerns. Recent research has shown that heavy rain events are projected to become more intense with climate change (e.g., Warner et al., 2015, Trenberth, 2011). This has altered the calculus regarding climate change impacts in the Pacific Northwest, since previous research suggested very little change in precipitation for the region. This is in part due to new methods of downscaling the large-scale changes projected by global climate models (GCMs) to smaller-scale changes of relevance to impacts assessment. Studies have shown that a physics-based approach (dynamical downscaling), is needed to capture changes in precipitation extremes and the associated impacts (Salathé et al., 2014). Previous approaches relied primarily on an empirical approach (statistical downscaling), which does not provide reliable estimates of changes in extremes. In dynamical downscaling, a regional climate model is used to simulate local-scale changes in climate, leading to a better representation of changes in the physical processes at these scales. This distinction is particularly important for precipitation, since dynamical downscaling can explicitly represent the interactions of weather systems with the complex terrain of the Pacific Northwest.

Regional weather and climate patterns can be influenced by conditions in other parts of the globe. As a result, regional climate model (RCM) simulations can only be produced by using the outputs from a global climate model as boundary conditions. Heavy rain events in the Pacific Northwest are typically driven by “Atmospheric River” (AR) events, in which narrow bands of concentrated moisture are carried into the region from lower latitudes. Previous studies have shown that global models are capable of representing the key aspects of Atmospheric Rivers (e.g., Flato et al., 2013), but lack the resolution to capture the local consequences for precipitation given the complex topography of the Pacific Northwest. This means that: (1) regional climate models are needed to estimate local-scale changes in extreme precipitation, and (2) global climate models are appropriate to use as boundary conditions for these regional climate simulations.

This task leverages a larger project, funded by King County, in which two new regional climate model projections were developed (Mauger et al., 2018).

Data & Methods

GCM Projections

Model	*Model Citation*	*Greenhouse Gas Scenario*	*Description*
ACCESS 1.0	Griffies et al., 2011	RCP 4.5 (Low emissions)	“Low-Low”
GFDL CM3	Bi et al., 2013	RCP 8.5 (High emissions)	"High-High”

Table 4. Model-Scenario pairs for the two global projections used to drive the regional model simulations. “Model” refers to the Global Climate Model (GCM, see Table 1 above), while “Scenario” refers to the greenhouse gas scenario (Van Vuuren et al., 2011, for more information see Section 1 of Mauger et al., 2015). These were chosen to bracket the range from a low-sensitivity model driven by a low-end greenhouse gas scenario (“Low-Low”) to a high-sensitivity model driven by a high-end greenhouse gas scenario (“High-High”).

We began by evaluating CMIP5 models for their ability to represent the climate and weather of the Pacific Northwest region. In particular, we developed a new set of model evaluation metrics aimed at evaluating models’ ability to capture the large-scale weather dynamics governing precipitation in the region. For example, one set of metrics considered the speed and location of the jet stream over the Northeast Pacific.

We then ranked the projections based on changes in precipitation extremes over the region. From the rankings we identified models that represented the low and high end of precipitation change for the region. Specifically, we selected the ACCESS 1.0 model with the RCP 4.5 scenario (“Low-Low”) and the GFDL CM3 model with the RCP 8.5 scenario (“High-High”) for downscaling with the regional climate model (Table 4).

Regional Climate Model (RCM) projections

Regional climate model simulations were performed using the Weather Research and Forecasting (WRF, http://www.wrf-model.org; Skamarock et al., 2005) community mesoscale model. WRF is a nonhydrostatic and mesoscale numerical weather model. Simulations were performed using WRF version 3.2 implemented following Salathé et al. (2010, 2014). Initial and boundary conditions were provided by the two model-scenario pairs identified above. Lateral boundary conditions and sea surface temperature (SST) were updated once every six hours.

Projections were downscaled to the region using two nested domains (Figure 3). The outermost domain at 36-km resolution covers the western North American continent and much of the eastern Pacific Ocean, in order to capture the climatological western flow and the evolution of approaching Atmospheric Rivers (ARs). The innermost domain, at 12-km resolution, encompasses the U.S.

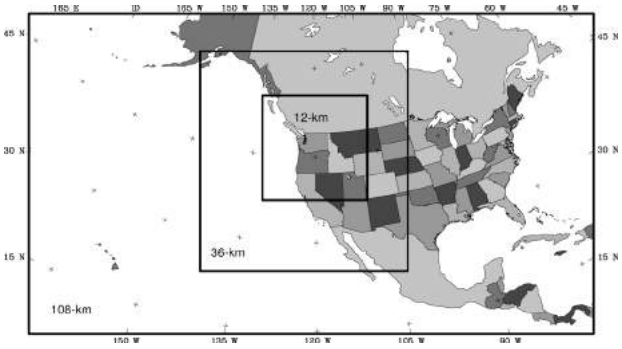

Figure 5. Domains for the WRF model: Western US at 36-km and Pacific Northwest at 12-km.

Pacific Northwest. One-way nesting was applied in this study. The model configuration is further summarized in Lorente et al. (2018). Although we did not perform an extensive validation of the model's performance, previous research has established that it captures the essential characteristics of local-scale weather variations in the Pacific Northwest (e.g., Dulière et al., 2011).

Simulations were performed for the years 1970 through 2099. Results were archived at hourly intervals following Greenwich Mean Time (GMT, which is 8 hours ahead of local standard time in the Pacific Northwest).

Observations

Hourly precipitation observations were obtained from Cooperative Observer Network (COOP) rain gauge sites through the NOAA National Center for Environmental Information (NCEI; NOAA 2003; see Table in Appendix B). COOP stations were selected based on the following criteria:

1. Over 30 years from start to end of observational record
2. At least 10% of available data has valid measurements
3. Observations continue through at least 1995

In all, there were 26 COOP stations in western Washington that met these criteria. Data were requested in mm. Although data for all gauges is included in the final results, the gauges highlighted in bold in Table B.3 are most pertinent to the current study.

Quality control procedures are described in Mauger et al. (2018). It is worth noting, however, that although we have made every attempt to comprehensively remove errors in the observations, some anomalous values may remain, and these errors could affect the bias correction of the model projections. For this reason, we have included extensive information on model biases, both before and after bias correction, in the products outlined below. In addition, we recommend using the percent changes from the raw projections as opposed to the absolute model projections whenever this is an option.

Bias Correction

Although WRF projections represent a substantial improvement over previous downscaled precipitation estimates, the simulations do contain biases. As a result, the raw WRF data were additionally bias-corrected to match the observations at each rain gauge site. To do so, we apply the "Percentile-Delta" method developed by Mauger et al. (2018). Described in detail in that publication, the method works by scaling the WRF data to match observed precipitation in each quantile range (i.e. 0-1, 1-2, … 99-100). The correction is applied to hourly data, and a separate set of adjustments is applied to the historical (1970-2005) and future (2006-2099) WRF simulations.

Statistics

Precipitation totals and extreme statistics were calculated for four 30-year time periods: 1970-1999 ("1980s"), 2020-2049 ("2030s"), 2040-2069 ("2050s"), and 2070-2099 ("2080s"). Although longer time periods might be desired to estimate extreme statistics, 30 years was deemed an appropriate compromise between longer periods, which may conflate long-term changes in flood risk with increased sampling of the extremes, and shorter time periods, which can limit the reliability of extremes estimates.

Since limited sample size can lead to errors in either the multi-year averages or extremes statistics, these were only calculated if the following conditions were met:

1. A minimum of 90% valid observations (< 10% missing values) to estimate the maximum or total for the water year or month in question.
2. A minimum of 5 years of valid observations to compute the long-term average (e.g., of total water year precipitation).
3. A minimum 10 years of valid observations to compute the 2-year extreme, and 25 years of valid data to compute the 5-, 10-, 25-, 50-, and 100-year extremes.

These conditions were chosen as a compromise between ensuring that the estimates are robust and the desire to include as many observational records as feasible in the analysis. Caution is advised regarding the results for the 50- and 100-year events, for which a 25-year record will likely be too short to produce robust estimates.

To calculate extreme statistics, we applied the GEV distribution with L-moments, following the methodology described in Salathé et al. (2014) and Tohver et al. (2014). Calculations were applied to multiple precipitation durations ranging from 1 hour to 15 days, and the precipitation intensities estimated for following recurrence intervals: 2-, 5-, 10-, 25-, 50-, and 100-year events (50%, 20%, 10%, 4%, 2%, and 1% annual chance of exceedance, respectively).

Results

All results from this study are available online and can be accessed via the links below. A Google Map has been created for identifying stations to facilitate navigation of the results directory. In addition, we have produced a series of summaries and visualizations that can be used to view the results.

- Direct link to results: http://cses.washington.edu/picea/mauger/2017_12_KingCounty_Stormwater/DATA/pub
- Google Map for locating stations: https://goo.gl/6rDsRH
- Interactive visualizations for viewing results: https://doi.org/10.7915/CIG4QJ78R

The interactive visualizations (Figure 6) include three separate viewers to allow users to view model biases relative to observations, view the percent changes for multiple recurrence intervals, and evaluate each of these for different precipitation durations. Additional details about the visualizations, data structure, and suggested interpretation of the results can be found in Mauger et al. (2018).

Figure 6. Screenshots of the three panels in the interactive visualization.

Summary & Interpretation

As an example, Table 5 shows the projected changes in the 1-hour precipitation statistics for the Quilcene 5 SW Dam rain gauge (COOP #456851). Projections for other precipitation durations and for the 2030s (2020-2049) and 2050s (2040-2069) are included in the data files available online.

Focusing on the 25-year event (4% annual chance of exceedance), Table 3 shows a –4 to +32% increase in the water year extreme. Seasonally, the simulations show the largest increase for spring and a tendency for decreases in summer, with a mixed response in fall. Although projected changes differ substantially among return intervals (2-yr event, 5-yr event, etc.), there is some consistency in the direction and magnitude of change.

A number of considerations are discussed in Mauger et al. (2018) that may be helpful to keep in mind when reviewing the projections. For convenience, these are summarized below:

- Projected changes will always be governed by a combination of random variability and long-term trends due to climate change. This is particularly true for changes in extremes: Since by definition these events are rare, it is difficult to accurately assess how rapidly they will change. Although even the 2080s projections can be significantly influenced by natural variability, we recommend focusing on these late century projections since this is when the projected changes will be largest relative to natural variability.

- The extremes estimates are limited by sample size. Whereas the 2- and 5-year events are relatively well captured in a 30-year record (e.g., 1970-1999, 2070-2099), extrapolation is needed to estimate the 50- and 100-year extremes. This means that the 50- and 100-year estimates are more prone to noise. For example, if the simulation includes one particularly large storm in the historical record, this could lead to artificially mute the projected change estimates even if, on average, most storms do become more intense. The converse is also true: a large storm at the end of the 21st century could artificially inflate the estimated change.

- Projected changes differ substantially for different precipitation durations. In general, changes appear to be largest for 1-hour precipitation and smallest for the longest durations. This is consistent with previous research projecting a change in atmospheric river events yet very little change in seasonal precipitation.

- As Table 5 suggests, the models do not correspond to the extremes among all GCMs and scenarios for all metrics and all times. In fact, the models do not generally correspond to their "Low" and "High" designations, which were based on an analysis of the regional drivers of precipitation. This is likely due to the distinct micro-climate of the northeast Olympic peninsula.

- Similarly, the two scenarios are unlikely to bracket the full range of potential future outcomes. Instead, these should be viewed as two equally-likely future projections which should be accounted for in planning and design. Future work can provide additional WRF simulations, from which we could obtain a more robust estimate of the mean and range among projections.

- The WRF model used in this study has a spatial resolution of 12 km. This is not enough to explicitly resolve convective precipitation, such as thunderstorms. Although these are represented statistically by the model, researchers generally consider that a finer resolution is needed to accurately capture convective events. This means that the current projections should be viewed primarily as an estimate of the change in the intensity of large-scale heavy precipitation events such as atmospheric rivers.

In this study, extremes were estimated by fitting a GEV distribution with L-moments (see "Statistics" section above). This approach will result in different estimates than the standard (e.g., Bulletin 17B, 1982) methods that are prescribed in certain applications. In most cases, these differences should be minor. However, we recommend repeating the calculations using the prescribed methodology to ensure consistent results and interpretation.

	Water Year		Dec-Feb		Mar-May		Jun-Aug		Sep-Dec	
	ACCESS 1.0 - RCP 4.5 (Low)	GFDL CM3 - RCP 8.5 (High)	ACCESS 1.0 - RCP 4.5 (Low)	GFDL CM3 - RCP 8.5 (High)	ACCESS 1.0 - RCP 4.5 (Low)	GFDL CM3 - RCP 8.5 (High)	ACCESS 1.0 - RCP 4.5 (Low)	GFDL CM3 - RCP 8.5 (High)	ACCESS 1.0 - RCP 4.5 (Low)	GFDL CM3 - RCP 8.5 (High)
Total	+15	-11	+16	-3	+10	-3	-56	-52	+23	-25
2-yr	+26	+9	+34	+25	+30	+12	-44	-20	+13	-7
5-yr	+32	+6	+35	+23	+40	+20	-40	-16	+24	-9
10-yr	+33	+2	+33	+21	+41	+23	-36	-15	+33	-10
25-yr	+32	-4	+30	+19	+39	+26	-30	-15	+48	-11
50-yr	+30	-9	+27	+17	+37	+27	-25	-16	+61	-11
100-yr	+28	-13	+24	+15	+34	+27	-19	-16	+74	-11

Table 5. Projected changes (%) in 1-hour precipitation statistics for the WRF grid point closest to the COOP Quilcene 5 SW Dam rain gauge (#456851), for the 2080s (2070-2099) relative to 1970-1999. Columns show the changes for both WRF scenarios for the full water year (Oct-Sep), as well as for winter (Dec-Feb), spring (Mar-May), summer (Jun-Aug), and fall (Sep-Dec). Rows show the projected change in the total accumulation for each time period as well as for the 2-, 5-, 10-, 25-, 50-, and 100-year events.

REFERENCES

Abatzoglou, J. T., & Brown, T. J. (2012). A comparison of statistical downscaling methods suited for wildfire applications. International Journal of Climatology, 32(5), 772-780. http://onlinelibrary.wiley.com/doi/10.1002/joc.2312/full

Bi D, Dix M, Marsland S, O'Farrell S, Rashid H, Uotila P, et al. The Access Coupled Model: Description, Control Climate and Evaluation. Australian Meteorological and Oceanographic Journal. 2013; 63:41-64. http://dx.doi.org/10.22499/2.6301.004

Brekke, L. D., Dettinger, M. D., Maurer, E. P., & Anderson, M. (2008). Significance of model credibility in estimating climate projection distributions for regional hydroclimatological risk assessments. *Climatic Change*, *89*(3-4), 371-394. http://dx.doi.org/10.1007/s10584-007-9388-3

(Bulletin 17-B) U.S. Interagency Advisory Committee on Water Data, 1982, Guidelines for determining flood flow frequency, Bulletin 17-B of the Hydrology Subcommittee: Reston, Virginia, U.S. Geological Survey, Office of Water Data Coordination, [183 p.]. [Available from National Technical Information Service, Springfield VA 22161 as report no. PB 86 157 278 or from FEMA at http://www.fema.gov/mit/tsd/dl_flow.htm

Daly, C., W. P. Gibson, G.H. Taylor, G. L. Johnson, P. Pasteris. 2002. A knowledge-based approach to the statistical mapping of climate. Climate Research, 22: 99-113

Daly, C., Halbleib, M., Smith, J.I., Gibson, W.P., Doggett, M.K., Taylor, G.H., Curtis, J., and Pasteris, P.A. 2008. Physiographically-sensitive mapping of temperature and precipitation across the conterminous United States. International Journal of Climatology, 28: 2031-2064..

Di Luzio, M., Johnson, G. L., Daly, C., Eischeid, J. K., & Arnold, J. G. (2008). Constructing retrospective gridded daily precipitation and temperature datasets for the conterminous United States. *Journal of Applied Meteorology and Climatology*, *47*(2), 475-497.

Dulière, V., Zhang, Y., & Salathé Jr, E. P. (2011). Extreme precipitation and temperature over the US Pacific Northwest: A comparison between observations, reanalysis data, and regional models. Journal of Climate, 24(7), 1950-1964.

Griffies, S. M., Winton, M., Donner, L. J., Horowitz, L. W., Downes, S. M., Farneti, R., ... & Palter, J. B. (2011). The GFDL CM3 coupled climate model: characteristics of the ocean and sea ice simulations. *Journal of Climate*, *24*(13), 3520-3544. https://doi.org/10.1175/2011JCLI3964.1

Hamlet, A. F. and D. P. Lettenmaier (2005) *Production of Temporally Consistent Gridded Precipitation and Temperature Fields for the Continental United States* Journal of Hydrometeorology, **6**, 330-336.

Hamlet, A.F., M.M. Elsner, G.S. Mauger, S-Y. Lee, I. Tohver, and R.A. Norheim. 2013. An overview of the Columbia Basin Climate Change Scenarios Project: Approach, methods, and summary of key results. *Atmosphere-Ocean* 51(4):392-415, doi: 10.1080/07055900.2013.819555.

Hegewisch,K.C., Abatzoglou J.T., 2016. An improved Multivariate Adaptive Constructed Analogs (MACA) Statistical Downscaling Method. *In preparation.*

Hosking, J. R. M., & Wallis, J. R. (2005). Regional frequency analysis: an approach based on L-moments. Cambridge University Press.

Kalnay, E., Kanamitsu, M., Kistler, R., Collins, W., Deaven, D., Gandin, L., ... & Zhu, Y. (1996). The NCEP/NCAR 40-year reanalysis project. Bulletin of the American meteorological Society, 77(3), 437-471.

King County (2018). *King County Standard Operating Procedures for Collection of Rainfall Data.* Department of Natural Resources and Parks, King County.

Kaufmann, P., & Weber, R. O. (1996). Classification of mesoscale wind fields in the MISTRAL field experiment. Journal of Applied Meteorology, 35(11), 1963-1979.

Livneh B., T.J. Bohn, D.S. Pierce, F. Munoz-Ariola, B. Nijssen, R. Vose, D. Cayan, and L.D. Brekke, 2015: A spatially comprehensive, hydrometeorological data set for Mexico, the U.S., and southern Canada 1950-2013, *Nature Scientific Data*, 5:150042, doi:10.1038/sdata.2015.42.

Livneh B., E.A. Rosenberg, C. Lin, B. Nijssen, V. Mishra, K.M. Andreadis, E.P. Maurer, and D.P. Lettenmaier, 2013: A Long-Term Hydrologically Based Dataset of Land Surface Fluxes and States for the Conterminous United States: Update and Extensions, *Journal of Climate*, 26, 9384–9392.

Lorente-Plazas, R., T. P. Mitchell, G. S. Mauger, E. P. Salathé Jr. (2018). Atmospheric rivers induce local extreme precipitation in the U.S. Pacific Northwest through interactions with the orography. *J. Hydrometeorology. In Review.*

Lynch, C.D. and G.S. Mauger. Consider the source: Ranking global models by evaluating the large-scale drivers of precipitation. *Manuscript in preparation.*

Mass, C. (1981). Topographically forced convergence in western Washington State. Monthly Weather Review, 109(6), 1335-1347.

Mauger, G.S., J.S. Won, K. Hegewisch, C. Lynch, R. Lorente Plazas, E. P. Salathé Jr. (2018). New Projections of Changing Heavy Precipitation in King County. Report

prepared for the King County Department of Natural Resources. Climate Impacts Group, University of Washington, Seattle.

Mauger, G.S., S.-Y. Lee, C. Bandaragoda, Y. Serra, J.S. Won, (2016). Refined Estimates of Climate Change Affected Hydrology in the Chehalis basin. Report prepared for Anchor QEA, LLC. Climate Impacts Group, University of Washington, Seattle. https://doi.org/10.7915/CIG53F4MH

Mauger, G.S., J.H. Casola, H.A. Morgan, R.L. Strauch, B. Jones, B. Curry, T.M. Busch Isaksen, L. Whitely Binder, M.B. Krosby, and A.K. Snover (2015). State of Knowledge: Climate Change in Puget Sound. Report prepared for the Puget Sound Partnership and the National Oceanic and Atmospheric Administration. Climate Impacts Group, University of Washington, Seattle. https://doi.org/10.7915/CIG93777D

Maurer, E. P., A. W. Wood, J. C. Adam, D. P. Lettenmaier, and B. Nijssen (2002) *A Long-Term Hydrologically Based Dataset of Land Surface Fluxes and States for the Conterminous United States,* Journal of Climate, **15**, 3237-3251.

Meehl, G. A., C. Covey, T. Delworth, M. Latif, B. McAvaney, J. F. B. Mitchell, R. J. Stouffer, and K. E. Taylor, 2007: The WCRP CMIP3 multi-model dataset: A new era in climate change

Miller, I.M., Morgan, H., Mauger, G., Newton, T., Weldon, R., Schmidt, D., Welch, M., Grossman, E. 2018. Projected Sea Level Rise for Washington State – A 2018 Assessment. A collaboration of Washington Sea Grant, University of Washington Climate Impacts Group, Oregon State University, University of Washington, and US Geological Survey. Prepared for the Washington Coastal Resilience Project.

Nick, M., Das, S. and Simonovic, S.P. 2011. The Comparison of GEV, Log-Pearson Type 3 and Gumbel Distributions in the Upper Thames River Watershed under Global Climate Models, the University of Western Ontario Department of Civil and Environmental Engineering, Report No:077. https://ir.lib.uwo.ca/wrrr/40/

North, G. R., Bell, T. L., Cahalan, R. F., & Moeng, F. J. (1982). Sampling errors in the estimation of empirical orthogonal functions. Monthly Weather Review, 110(7), 699-706.

(NOAA) U.S. Department of Commerce, National Oceanic and Atmospheric Administration, National Centers for Environmental Information (NCEI). (2003). *DATA DOCUMENTATION FOR DATA SET 3240 (DSI-3240); Hourly Precipitation Data*. https://www.ncdc.noaa.gov/IPS/hpd/hpd.html

National Research Council Report on Sea Level Rise in California, Oregon and Washington includes absolute sea level contributions of GIA ranging between -1.04 to 0.37 mm/yr. The report is available at:

https://www.nap.edu/catalog/13389/sea-level-rise-for-the-coasts-of-california-oregon-and-washington

Port Gamble S'Klallam Tribe Natural Resources Department. 2017. Climate Change Impact Assessment. A collaboration of the Port Gamble S'Klallam Tribe, Cascadia Consulting Group, and the University of Washington Climate Impacts Group.

Rahman, A., Weinmann, P.E. and Mein, R.G. (1999). At-site flood frequency analysis: LP3-product moment, GEV-L moment and GEV-LH moment procedures compared. In: Proceeding Hydrology and Water Resource Symposium, Brisbane, 6–8 July, 2, 715–720.

Rahman, A., Karin, F, and Rahman, A. 2015. Sampling Variability in Flood Frequency Analysis: How Important is it? 21st International Congress on Modelling and Simulation, Gold Coast, Australia, Nov 29-Dec 4, 2015, 2200-2206.

Ramirez, M.F. and Simenstad, C.A. 2018. Projections of Future Transitions in Tidal Wetlands under Sea Level Rise within the Port Gamble S'Klallam Traditional Use Areas. Report prepared for the Port Gamble S'Klallam Tribe. School of Aquatic and Fishery Sciences, University of Washington, Seattle. http://depts.washington.edu/wet/research/Tidal%20Wetland%20Response%20to%20SLR_Final%20Report.pdf

Roeckner, E., Bäuml, G., Bonaventura, L., Brokopf, R., Esch, M., Giorgetta, M., et al. (2003). The atmospheric general circulation model ECHAM 5. PART I: Model description.Report / MPI für Meteorologie, 349.

Rupp, D. E., Abatzoglou, J. T., Hegewisch, K. C., & Mote, P. W. (2013). Evaluation of CMIP5 20th century climate simulations for the Pacific Northwest USA. *Journal of Geophysical Research: Atmospheres*, *118*(19).

Ryoo, J. M., Y. Kaspi, D. W. Waugh, G. N. Kiladis, D. E. Waliser, E. J. Fetzer, and J. Kim, (2013). Impact of Rossby Wave Breaking on U.S. West Coast Winter Precipitation during ENSO Events. *J. Climate*, 26, 6360-6382.

Salathé Jr., Eric P., Alan F. Hamlet, Clifford F. Mass, Se-Yeun Lee, Matt Stumbaugh, and Richard Steed, 2014: Estimates of Twenty-First-Century Flood Risk in the Pacific Northwest Based on Regional Climate Model Simulations. J. Hydrometeor, 15, 1881–1899. doi: http://dx.doi.org/10.1175/JHM-D-13-0137.1

Scheff, J., & Frierson, D. M. (2012). Robust future precipitation declines in CMIP5 largely reflect the poleward expansion of model subtropical dry zones. Geophysical Research Letters, 39(18).

Siler, N., & Durran, D. (2016). What causes weak orographic rain shadows? Insights from case studies in the Cascades and idealized simulations. Journal of the Atmospheric Sciences, 73(10), 4077-4099.

Sillmann, J., V. V. Kharin, F. W. Zwiers, X. Zhang, and D. Bronaugh, 2013a: Climate extremes indices in the CMIP5 multimodel ensemble: Part 2. Future climate projections. *Journal of Geophysical Research Atmos.*, **118**: 2473–2493, http://dx.doi.org/10.1002/jgrd.50188

Sillmann, J., V. Kharin, X. Zhang, F. Zwiers, and D. Bronaugh, 2013b: Climate extremes indices in the CMIP5 multimodel ensemble: Part 1. Model evaluation in the present climate. *Journal of Geophysical Research: Atmospheres*, **118**(4): 1716-1733. http://dx.doi.org/10.1002/jgrd.50203

Taylor, K. E. et al., 2012. An overview of CMIP5 and the experiment design. *Bulletin of the American Meteorological Society*, *93*(4), 485-498, doi:10.1175/BAMS-D-11-00094.1

Tohver, I. M., Hamlet, A. F., & Lee, S. Y. (2014). Impacts of 21st-Century Climate Change on Hydrologic Extremes in the Pacific Northwest Region of North America. JAWRA Journal of the American Water Resources Association, 50(6), 1461-1476. https://doi.org/10.1111/jawr.12199

Trenberth, K. E. (2011). Changes in precipitation with climate change. Climate Research, 47(1-2), 123-138. http://dx.doi.org/10.3354/cr00953

Van Vuuren, D., J. Edmonds, M. Kainuma, K. Riahi, A. Thomson, K. Hibbard, G. Hurtt, T. Kram, V. Krey, J. Lamarque, T. Masui, M. Meinshausen, N. Nakicenovic, S. Smith, S. Rose, 2011: The representative concentration pathways: an overview. *Climatic Change*, **109**: 5-31. http://dx.doi.org/10.1007/s10584-011-0148-z

Vogel, R.M., McMahon, T.A. and Chiew, F.H.S. (1993). Flood flow frequency model selection in Australia, Journal Hydrology, 146, 421-449. https://doi.org/10.1016/0022-1694(93)90288-K

Ward Jr, J. H. (1963). Hierarchical grouping to optimize an objective function. Journal of the American statistical association, 58(301), 236-244.

Warner, M. D., Mass, C. F., & Salathé Jr, E. P. (2015). Changes in winter atmospheric rivers along the North American west coast in CMIP5 climate models. *Journal of Hydrometeorology*, *16*(1), 118-128. https://doi.org/10.1175/JHM-D-14-0080.1

Wilks, D. (1995). Statistical Methods in Atmospheric Sciences: An Introduction. Academic Press.

Appendix A: Scope of Work

EXHIBIT A:
Scope of Services

The Services to be performed by University of Washington key personnel at the Climate Impacts Group (CIG) and the School of Aquatic and Fisheries Sciences (SAFS), on the Project shall be as described below and shall be performed pursuant to the Project Schedule set out below.

Task A. Review impact assessment chapters from a science perspective

CIG will also be asked to review each chapter (drafted by Cascadia) from a science perspective. These may include, for example, chapters covering climate change impacts on human health & safety, mammals, water quality and quantity, sea level rise, shorelands, and/or other resources or sectors.

The CIG has been allocated approximately 20 hours for this task ($1,520). This will be reported under **Task 3** in Cascadia's invoice to the client.

Task B. Synthesize and statistically downscale global climate model projections

Climate projections for Pacific Northwest temperature, precipitation, and sea level rise through 2100 are currently available in the existing literature on Pacific Northwest climate change impacts; projections beyond 2100 have not been produced for the region. Through this task, the UW/CIG will produce long-range projections of changing temperature, precipitation, and sea level through to the year 2160 (which spans seven generations), for use by the Port Gamble S'Klallam Tribe in planning efforts.

The two sub-tasks will consist of obtaining and summarizing global climate model projections for Western Washington through 2160. This includes bias correcting and localizing the global climate model output by statistically downscaling the projections to select observing stations that are in close proximity to Tribal lands.

2.1 Synthesize global climate model projections. UW will synthesize existing global climate model projections of temperature and precipitation through the year 2160 for a region that encompasses the tribe's historical lands (e.g., Western Washington). Projections will be obtained from the new suite of global model projections available through the Climate Model Inter-comparison Project, phase 5 (CMIP5[1]). Simulations will be implemented using the high-end, "business as usual," RCP 8.5 (Representative Concentration Pathway[2]) and the low-end RCP 4.5 greenhouse gas scenario. Projections will be summarized for annual and seasonal temperature and precipitation, and the results will be summarized to highlight the average, minimum, and maximum change projected, as well as the time evolution of changes projected by each of the models from the late 1900s through 2160. In addition to summarizing the global climate model output, the final report will summarize previous literature evaluating each model's ability to accurately simulate the climate of the Pacific Northwest and discuss the relative merits and limitations of the data available for post-2100 projections.

2.2 Statistically downscale global climate model projections. The global model projections obtained in sub-task 2.1 will then be "downscaled" to specific locations selected to be in or near Tribal lands. This step will involve relating measurements from select high-quality weather stations to large-scale variations

[1] Taylor, K. E. et al., 2012. An overview of CMIP5 and the experiment design. *Bulletin of the American Meteorological Society*, *93*(4), 485-498, doi:10.1175/BAMS-D-11-00094.1

[2] Van Vuuren, D. P. et al., 2011. The representative concentration pathways: An overview. *Climatic Change*, 109(1-2), 5-31.

Appendix B: Precipitation Gauges

Station Name	*ID*	*Location*	*Dates*	*Yrs*
BURLINGTON	450986	48.46720N / 122.31360W	07/04/1948--01/01/2014	65
CLEARWATER	451496	47.57110N / 124.29220W	07/01/1948--01/01/2014	65
COUGAR 4 SW	451759	46.00860N / 122.34550W	07/01/1948--01/01/2014	65
CUSHMAN DAM	451934	47.42380N / 123.21970W	07/19/1948--01/01/2014	65
EVERETT	**452675**	**47.97520N / 122.19500W**	**07/04/1948--01/01/2014**	**65**
MARBLEMOUNT RANGER STATION	454999	48.53800N / 121.45020W	07/06/1948--01/01/2014	65
QUILCENE 5 SW DAM	**456851**	**47.78470N / 122.97970W**	**09/26/1948--01/01/2014**	**65**
SNOQUALMIE PASS	457781	47.42470N / 121.41380W	07/01/1948--09/01/2013	65
SPOKANE INTERNATIONAL AIRPORT	457938	47.62160N / 117.52800W	08/01/1948--12/30/2013	65
STAMPEDE PASS	458009	47.27670N / 121.33720W	07/01/1948--12/31/2013	65
PALMER 3 ESE	456295	47.30580N / 121.85130W	07/01/1948--02/01/2013	64
MUD MOUNTAIN DAM	455704	47.14130N / 121.93550W	07/04/1948--02/01/2010	61
PORT ANGELES	**456624**	**48.11380N / 123.43160W**	**07/01/1948--11/01/2008**	**60**
MONTESANO 1 S	455549	46.96750N / 123.60640W	08/01/1954--01/01/2014	59
OLYMPIA AIRPORT	456114	46.97330N / 122.90330W	08/15/1954--12/31/2013	59
SNOQUALMIE FALLS	457773	47.54130N / 121.83610W	08/01/1954--09/01/2013	59
LANDSBURG	454486	47.37660N / 121.96130W	08/01/1954--02/01/2013	58
ABERDEEN 20 NNE	450013	47.26130N / 123.71470W	07/01/1948--11/02/2004	56
CEDAR LAKE	451233	47.41440N / 121.75610W	08/01/1953--01/01/2010	56
CARNATION 4 NW	451146	47.69306N / 121.99472W	07/04/1948--02/01/2003	54
WESTPORT 2 S	459112	46.87083N / 124.10833W	08/05/1948--03/01/2003	54
GREENWATER	453357	47.13333N / 121.63333W	07/04/1948--01/01/1999	50
SAPPHO 8 E	457319	48.06667N / 124.11667W	07/04/1948--04/01/1998	49
SEATTLE TACOMA INTERNATIONAL AIRPORT	457473	47.44440N / 122.31380W	01/01/1965--12/31/2013	49
QUILLAYUTE STATE AIRPORT	456858	47.93750N / 124.55500W	08/01/1966--12/31/2013	47
GRAYS RIVER	453329	46.36667N / 123.56667W	08/01/1954--05/01/1991	36
SEATTLE PORTAGE BAY	457458	47.65000N / 122.30000W	03/01/1973--07/01/1998	25

Table B.1. NOAA Cooperative (COOP) Network Rain Gauges used in this study. Gauges are listed in order from longest to shortest observational record. Stations that are closest to PGSK headquarters are highlighted in bold.